RSC Advances

PAPER

View Article Online
View Journal | View Issue

Cite this: *RSC Adv.*, 2014, **4**, 54879

The effect of electric field on hydrogen storage for B/N-codoped graphyne†

Lihong Zhang,[a] Ning Wang,[a] Shengli Zhang[b] and Shiping Huang*[a]

Received 29th July 2014
Accepted 8th October 2014

DOI: 10.1039/c4ra07761j

www.rsc.org/advances

Hydrogen adsorption on a B/C/N sheet under different external electric fields is investigated by first-principles calculations. Through the analyses of structural properties of the B/C/N system, we find that N_bB_f, B_bN_o, B_aN_e, and N_aB_g are more probable to be synthesized. Through molecular dynamics calculations, it was found that the structures for B/N doped graphyne are stable. For N_bB_f, B_bN_o, B_aN_e, and N_aB_g, the most stable positions for hydrogen adsorption are the H1 sites. For a single H_2 adsorbed on a B/C/N sheet, the adsorption energy increases greatly as the electric field increases, and the maximum adsorption energy is 0.506 eV when the electric field is 0.035 a.u. It is also found that the adsorption energy of H_2 adsorbed on N_bB_f under electric field increases faster than H_2 adsorbed on other sheets. The interaction between H_2 molecule and B/C/N sheet is the Kubas interaction under an external electric field.

1. Introduction

Due to rising standards of living and growing populations, energy consumption is expected to increase dramatically. Hydrogen is very attractive as a clean energy source because of its efficiency, abundance and environmental friendliness.[1–4] However, how to store hydrogen safely and transport efficiently is a crucial problem.[3,5]

Among various hydrogen storage materials, carbon-based nanostructures, including nanotubes,[6] fullerenes[7] and graphenes, have attracted considerable attention because of their remarkable properties, such as good reversibility, high capacity, and fast kinetics.[8] However, hydrogen adsorption on carbon materials is limited by the van der Waals (vdW) interaction, which is too weak to store hydrogen in moderate conditions. Recent studies showed that nanostructures composed of light elements such as B and N offer many advantages to store hydrogen.[9–11] For example, the BN layer is slightly more resistant to oxidation than graphene, and is thus more suitable for application at room temperature, where graphene would be oxidized.[12] Furthermore, similar to carbon nanotubes, BN nanotubes are also regarded as possible hydrogen storage media. It has been experimentally found that the BN nanotubes can store as much as 2.6 wt% of hydrogen at 10 MPa.[13] Collapsed BN nanotubes exhibit a higher hydrogen storage capacity with 4.2 wt% of hydrogen.[14] Moreover, Zhou *et al.* pointed out that an effective method to promote hydrogen adsorption is to add an external electric field.[9] The new concept is based on the fact that the polarization of H_2 molecule caused by the electric field associated with point ions allows exposed metal cations to store hydrogen in a quasi-molecular form.[15,16] Subsequently, Liu *et al.* put forward that electric field can induce a reversible switch for hydrogen adsorption and desorption based on Li-doped carbon nanotube and Li-doped graphene.[17,18] Enhanced hydrogen adsorption on carbonaceous sorbent under an electric field has been demonstrated in experiment by Shi *et al.*[19]

Currently, there are some theoretical reports examining graphyne. Graphyne is a new carbon-based form that consists of planar carbon sheets containing sp and sp^2 bonds,[20–23] which can be regarded as the big hexagonal rings joined together by the acetylenic linkages (C–C≡C–C) rather than the C–C=C–C in graphene. Experimentally, although large graphyne structures have not been synthesized yet, graphdiyne (expanded graphynes) films and graphdiyne tubes have been already obtained.[24]

In this study, we present theoretical study of the structure of 2D graphyne and its structural analogs involving BN rings (BN-yne). The latter is composed of BN hexagonal rings linked by C-chains. In this work, we investigate the stability of B/C/N systems, structural characteristic and electronic properties of hydrogen adsorption on a B/C/N sheet using density functional theory (DFT) calculations. First, we study the possible synthesis for B/C/N system based on the formation energy of B/C/N sheet. Then, we investigate stability of the B/C/N sheets through a dynamic calculation. Finally, we focus on the structural and electronic characteristics of hydrogen adsorption on the B/C/N sheet under different electric fields.

[a]*State Key Laboratory of Organic-Inorganic Composites, Beijing University of Chemical Technology, Beijing 100029, China. E-mail: huangsp@mail.buct.edu.cn; Fax: +86-10-64427616*

[b]*School of Materials Science and Engineering, Nanjing University of Science and Technology, Nanjing, Jiangsu, 210094, China*

† Electronic supplementary information (ESI) available. See DOI: 10.1039/c4ra07761j

2. Computational methods

All geometry optimizations are carried out using DFT calculations within the local density approximation (LDA) as implemented in the DMol3 package.[25,26] We applied the Perdew and Wang correlation functional (PWC)[27] and relaxed the geometries. Previous studies have demonstrated that LDA can predict the physisorption energies of H_2 on the surface of graphite and carbon nanotubes accurately[28–30] and can be suitable for charged carbon nanostructures with electric fields.[17,31] Full structural optimizations were obtained using a convergence tolerance energy of 1×10^{-5} Hartree, a maximum force of 2×10^{-3} Hartree per Å, and a maximum displacement of 5×10^{-3} Å. Moreover, a double numerical-polarized basis set (DNP) is employed. The DNP basis set included a double quality basis set with a p-type polarization function added to hydrogen and d-type polarization functions added to heavier atoms. Self-consistent field (SCF) calculations were performed with a convergence of 1×10^{-6} Hartree on the total energy. The direct inversion of iterative subspace (DIIS) approach was used to accelerate SCF convergence. A (2×2) B/N-codoped graphyne supercell was established with lattice parameters of $a = b = 13.7887$ Å, $c = 28.7497$ Å, $\alpha = \beta = 90°$, $\gamma = 120°$. The vacuum space of 20 Å was used in the direction perpendicular to the B/C/N sheet in order to avoid the interaction between neighboring layers. The electric field was applied in the z direction, as shown in Fig. 1. The total density of states (DOS) and partial density of states (PDOS) of B/N-doped graphyne with and without electric field in the super cells were calculated with a k-point of $(12 \times 12 \times 1)$. The Ortmann, Bechstedt and Schmidt (OBS) method was employed to correct the dispersion effect,[32] and the effect of basis set superposition error (BSSE) was considered with the use of counterpoise (CP) correction.[33]

3. Results and discussion

The optimized structure of pristine graphyne is shown in Fig. 2. In pristine graphyne, the bonds of C atoms have three types, *i.e.*, C–C single bond, C=C double bond, and C≡C triple bond (marked as number 1, 2, and 3 in Fig. 2, respectively). The bond lengths of C–C, C=C, and C≡C are 1.410 Å, 1.430 Å, and 1.227 Å, respectively. The calculated bond lengths are in good agreement with previous reports.[28,34] For B- or N-doped graphyne, there are two inequivalent sites for one B or N atom randomly substituting one C atom in graphyne, labeled as *a* and *b* in Fig. 2. After the structure optimization, the geometries are obtained and their structural parameters are presented in Table 1. The formation energy (E_F) can be defined as follows:

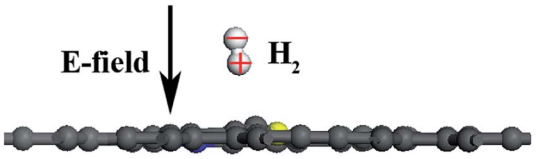

Fig. 1 Single H_2 adsorbed on the N_bB_f sheet, vertical electric field is applied in the z direction.

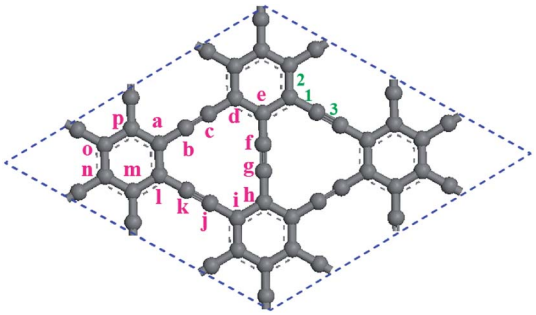

Fig. 2 The optimized structure of pristine graphyne. Numbers 1, 2, and 3 donate C–C, C=C, and C≡C bonds, respectively; Letters a, b, …, p represent 16 substitution positions for B(N) doping and B/N codoping.

Table 1 The bond lengths of C–B (C–N), and the formation energies E_F for B or N doping

	B doping		N doping	
	a site	b site	a site	b site
$d_{C-B(N)}$ (Å)	1.528, 1.492	1.485, 1.344	1.423, 1.357	1.366, 1.187
E_F (eV)	0.23	0.19	0.15	0.19

$$E_F = E_{DG} + nE_C - E_{PG} - \sum E_{Dopant} \quad (1)$$

where E_{DG} is the total energy of single doped or codoped graphyne, E_{PG} is the total energy of pristine graphyne, and $\sum E_{Dopant}$ is the total energy of dopant B, N, or B/N pairs. E_C is the energy of one carbon atom in pristine graphyne, and n is the number of carbon atoms substituted by dopants. In the case of B doping at a site, the bond lengths of three B–C bonds are 1.528, 1.528, and 1.492 Å, longer than corresponding d_{C-C} in pristine graphyne. For N doping, the bond lengths of the three N–C bonds are 1.423, 1.423, and 1.357 Å, which are equal or shorter than corresponding d_{C-C} in pristine graphyne. In the case of B (N) doping at the b site, the bond lengths of B–C are 1.485 and 1.344 Å, longer than the corresponding d_{C-C} in pristine graphyne; the bond lengths of N–C are 1.366 and 1.187 Å, shorter than the corresponding d_{C-C} in pristine graphyne. In a word, the bond lengths of B–C (N–C) are longer (shorter) than the bond lengths of corresponding C–C bonds in the case of both B(N) doping at the *a* site and *b* site, due to different atomic radius of B and N atoms. It can be seen from the formation energy (in Table 1) that B or N doped at the *a* site and *b* site of graphyne are of great possibility to be synthesized, especially for N-doped graphyne.

As for B/N codoping, we considered sixteen substitution sites. We divided the codoping configurations into two groups, as shown in Fig. 2. One is ax or xa (x = b, c, …, p), which represents that B (or N) atom substitutes C atom in a site and N (or B) atom substitutes C atom in b, c, d, e, f, g, h, i, j, k, l, m, n, o, and p sites; the other is by or yb (y = a, c, d, …, p), which indicates that B (or N) atom substitutes C atom in b site and N (or B) atom substitutes C atom in a, c, d, e, f, g, h, i, j, k, l, m, n, o, and p sites. As given in Table 2, the d_{C-B} and d_{C-N} for B/N

Table 2 The C-dopants distance (d_{C-B} and d_{C-N}), and the formation energy (E_F). When B or N atom bond with several C atoms, the d_{C-B} or d_{C-N} indicate the shortest bond length. (The definitions of all symbols can be seen in Fig. 2)

ax	ab	ac	ad	ae	af	ag	ah	ai	aj	ak	al	am	an	ao	ap
d_{C-B} (Å)	1.521	1.512	1.504	1.497	1.490	1.490	1.488	1.491	1.489	1.488	1.491	1.492	1.493	1.492	1.494
d_{C-N} (Å)	1.179	1.172	1.344	1.355	1.187	1.186	1.355	1.348	1.185	1.179	1.352	1.406	1.405	1.415	1.405
E_F (eV)	0.265	0.237	0.196	0.190	0.228	0.227	0.193	0.191	0.240	0.235	0.233	0.233	0.196	0.200	0.197
xa	ba	ca	da	ea	fa	ga	ha	ia	ja	ka	la	ma	na	oa	pa
d_{C-B} (Å)	1.348	1.342	1.504	1.490	1.346	1.345	1.489	1.495	1.346	1.343	1.490	1.526	1.521	1.526	1.520
d_{C-N} (Å)	1.415	1.315	1.344	1.348	1.354	1.353	1.355	1.354	1.352	1.355	1.352	1.353	1.355	1.350	1.354
E_F (eV)	0.189	0.156	0.196	0.191	0.152	0.150	0.193	0.190	0.162	0.153	0.232	0.233	0.196	0.200	0.196
by	ba	bc	bd	be	bf	bg	bh	bi	bj	bk	bl	bm	bn	bo	bp
d_{C-B} (Å)	1.348	1.513	1.342	1.347	1.344	1.344	1.345	1.346	1.342	1.344	1.343	1.343	1.348	1.351	1.348
d_{C-N} (Å)	1.415	1.337	1.315	1.352	1.185	1.187	1.352	1.354	1.187	1.187	1.355	1.411	1.416	1.425	1.417
E_F (eV)	0.189	0.271	0.156	0.162	0.190	0.192	0.150	0.152	0.188	0.189	0.153	0.153	0.153	0.141	0.153
yb	ab	cb	db	eb	fb	gb	hb	ib	jb	kb	lb	mb	nb	ob	pb
d_{C-B} (Å)	1.521	1.512	1.514	1.488	1.343	1.344	1.490	1.490	1.344	1.344	1.487	1.527	1.532	1.531	1.530
d_{C-N} (Å)	1.179	1.337	1.173	1.184	1.187	1.187	1.186	1.188	1.185	1.187	1.180	1.179	1.182	1.175	1.182
E_F (eV)	0.265	0.271	0.237	0.240	0.188	0.192	0.227	0.228	0.190	0.189	0.234	0.235	0.230	0.222	0.230

codoping are almost the same as those of single B and N doping, indicating that the configuration maintains the planar structure.[35] The formation energies changed from 0.190 to 0.265 eV for ax and from 0.150 to 0.233 eV for xa, indicating that N doping at a site is easier to synthesize than B doping at a site; the formation energies vary from 0.141 to 0.271 eV for bx and from 0.188 to 0.271 eV for xb, revealing that B doping at the b site is easier to synthesize than N doping at b site.

To check the stability of B/C/N system, we use the *ab initio* molecular dynamics (MD) simulation for B/C/N sheets. In the simulations, the temperature gradually increases from 1 to 900 K in 1000 time steps, and the time step is 1 fs. It is found that the structure does not undergo an evident deformation even at the temperature of 900 K.

Based on the formation energy, we choose four B/N-codoping configurations to investigate one H_2 adsorbed on different sites of B/C/N sheets. There are three types of adsorption sites on B/C/N sheets: hollow site (H), top site (T), and bridge site (B). For N_bB_f, there are two hollow sites, five top sites, and five bridge sites, as shown in Fig. 3(a). The calculated results of adsorption energies are summarized in Fig. 3(b). The adsorption energy of H_2 on B/C/N sheets is defined as follows:

$$E_{ad} = E^F_{B/C/N} + E^F_{H_2} - E^F_{H_2-B/C/N} \quad (2)$$

where $E_{H_2-B/C/N}$ is the total energy of H_2 adsorbed on the B/C/N sheets, $E_{B/C/N}$ is the total energy of B/C/N sheets, and E_{H_2} is the total energy of free-standing H_2 molecule. F indicates the intensity of electric field; when $F = 0$, eqn (2) refers to the E_{ad} without the electric field; when $F \neq 0$, eqn (2) refers to the E_{ad} under the electric field. Dispersion and BSSE corrections are introduced to the calculation, and these correction data are listed in the ESI Table S1.† It can be seen that the largest

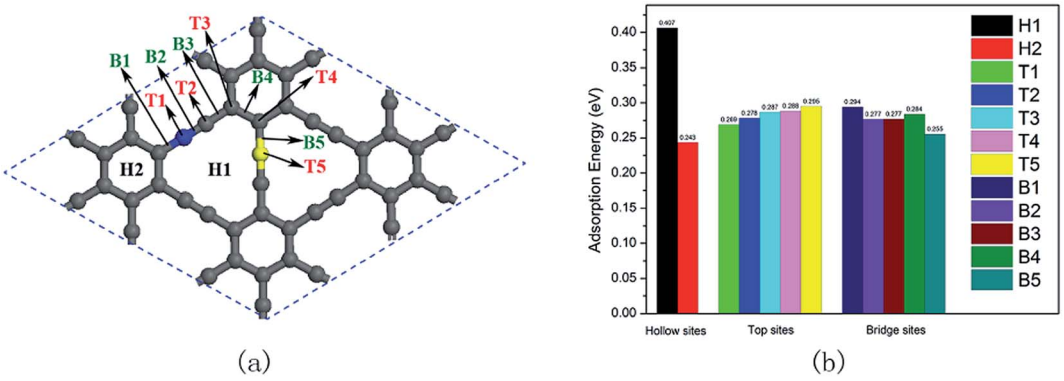

Fig. 3 (a) Different adsorption sites on a N_bB_f sheet, including two hollow sites (H), five top sites (T), and five bridge sites (B). The gray, blue, and yellow balls are carbon, nitrogen, and boron atoms, respectively. (b) The adsorption energy of H_2 adsorbed on different sites of N_bB_f sheet with DFT-D and BSSE correction.

adsorption energy of H_2 adsorbed on N_bB_f is 0.407 eV at the H1 site. Then, we calculate the adsorption energies of H_2 adsorbed on different sites of B_bN_o, B_aN_e, and N_aB_g sheets, and the most favorable positions are the H1 site with the largest adsorption energies of 0.400, 0.357, and 0.341 eV, respectively.

Then we studied the relative stability of different configurations for H_2 molecule on the B/C/N sheet in an external electric field vertical to the sheet. Similar to the field-free case, three types of adsorption sites (top site, bridge site, and hollow site) were considered. For each site, various initial orientations of the H_2 molecule were studied. After optimization, it was seen that the angle between H_2 molecule and B/N-codoped graphyne plane increases with the increase of electric field, as shown in Fig. 4. The H_2 molecule prefers to align along the *z* direction, *i.e.* parallel to the electric field, when the intensity of the electric field is strong enough, for example, 0.035 a.u. in the case of single H_2 absorbed on the N_bB_f sheet. For N_bB_f, B_bN_o, B_aN_e, and N_aB_g, the preferable positions are H1 sites; for N_a and N_b, the preferable positions are T4 and H2 sites.

We also investigated the effect of the electric field on hydrogen adsorption. As shown in Fig. 5, the hydrogen adsorption energy and the H–H bond length are plotted as a function of the magnitude of the electric field. Both dispersion and BSSE corrections are considered in the calculation, as listed in the ESI Table S2.† It can be found that the adsorption energy increases dramatically under the electric field, indicating that the electric field can easily modulate the adsorption energy of H_2 adsorbed on the B/C/N sheet. It is also found that the adsorption energy of H_2 adsorbed on N_bB_f under an electric field increases faster than H_2 adsorbed on other sheets. Through Mulliken charge analysis in Table 3, we find that the charge of the B/C/N sheets increases with increasing the electric field strength, whereas the increase for electric quantity of N_bB_f is faster than other sheet. This may be considered for why the adsorption energy of H_2 adsorbed on N_bB_f increases faster than H_2 adsorbed on other sheets. Due to the polarization interaction induced by the electric field and the polar bonds on the B/C/N sheets, the H–H bond length increased greatly with increasing electric field strength. When the electric field reached 0.038 a.u., the H–H bond length became 0.870 Å for H_2 adsorbed on a N_bB_f sheet, and an elongation of nearly 13% occurred. It has been reported that the Kubas interaction between a transition metal atom and H_2 can elongate the bond length by 10–25%.[36,37] The interaction energy between H_2 molecule and B/N-codoped graphyne are in the range of 0.243–0.407 eV in absence of an electric field. However, the interaction energy was in the range of 0.407–0.506 eV in presence of an electric field. These results illustrate the interaction between H_2

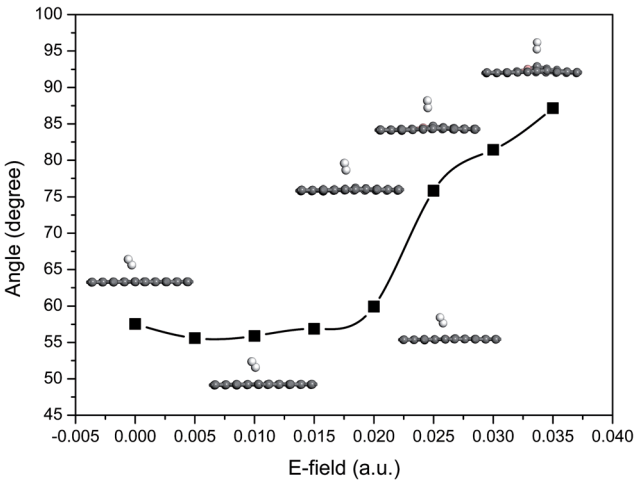

Fig. 4 The configurations of single H_2 absorbed on the N_bB_f sheet, with the increase of electric field. The vertical coordinate represents the angle between H_2 molecule and B/N-codoped graphyne plane.

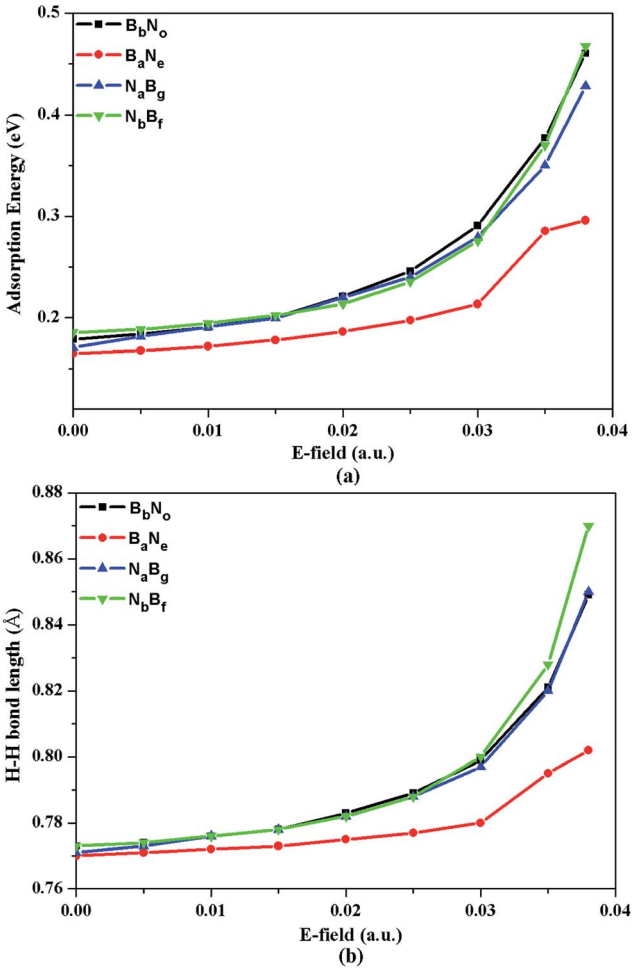

Fig. 5 (a) The adsorption energy and (b) the H–H bond length as a function of the magnitude of the electric field.

Table 3 The change of the Mulliken charge for the B/C/N sheets under the electric field

	The Mulliken charge for B/C/N sheets (|e|)			
E-field (a.u.)	B_bN_o	B_aN_e	N_aB_g	N_bB_f
0	0.012	0.010	0.007	0.010
0.02	0.049	0.026	0.044	0.048
0.035	0.143	0.077	0.143	0.155

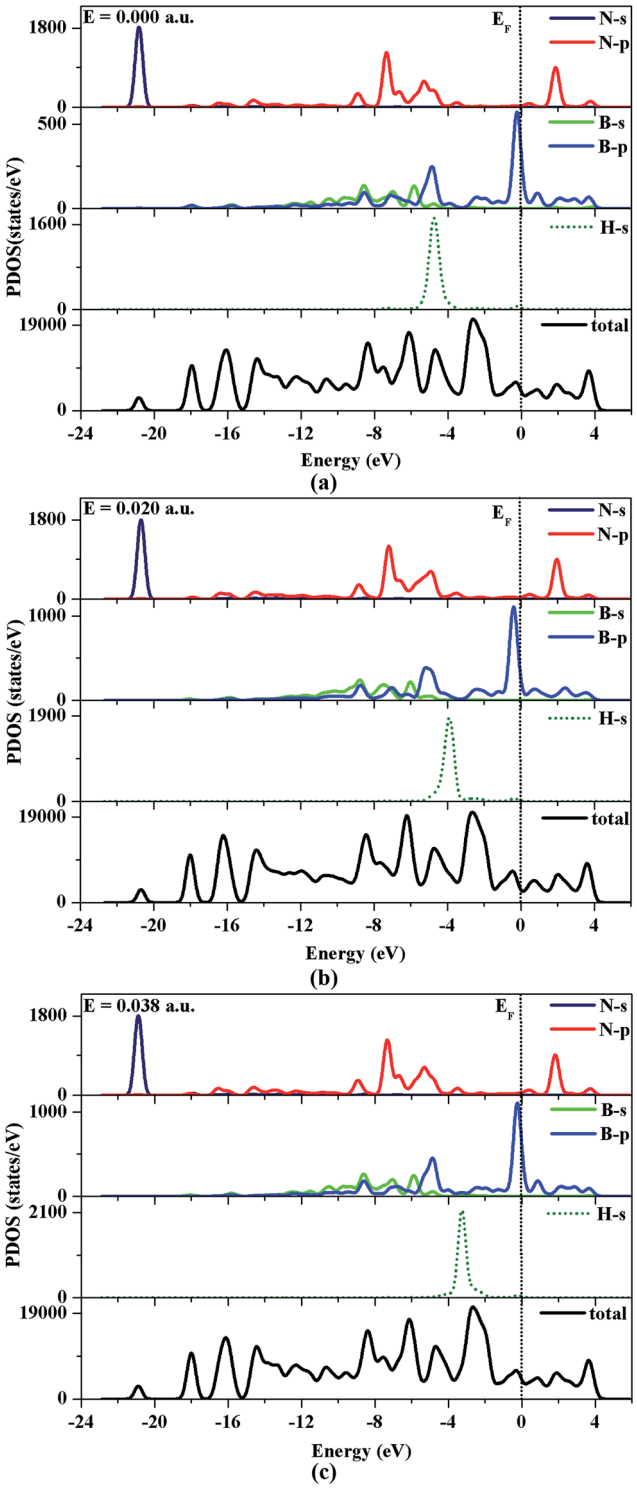

Fig. 6 The partial density of states for one single H_2 adsorbed on N_bB_f under different electric fields. (a) The electric field is 0.000 a.u. (b) The electric field is 0.020 a.u. (c) The electric field is 0.038 a.u. The Fermi energy is set to zero.

molecule and B/N-codoped graphyne is the Kubas interaction. From the analysis of molecular orbitals, it was found that the bonding orbitals are mainly between the π orbital of the B/N-codoped graphyne and the σ* anti-bonding orbital of the hydrogen molecule, and this interaction can be explained by the Kubas interaction.[35] When the electric field intensity is 0.039 a.u., we found that the H_2 molecule was dissociated. Therefore, the molecular hydrogen adsorption can be achieved only under a certain electric field.

To investigate the effect of the electric field on the electronic structure, we analyzed the partial density of states (PDOS) for a single H_2 adsorbed on B/C/N sheets under different electric fields. Fig. 6 shows the PDOS of the hydrogen atom, boron atom and nitrogen atom for H_2 adsorbed on N_bB_f. We found that the H-s orbital moved toward the Fermi level as the electric field strength was increased. This indicates that the H_2 elongated by the electric field was less stable than the free-H_2 molecule.

4. Conclusions

DFT calculations were carried out to explore the B/N-codoped graphyne for hydrogen storage. Through the analyses of the structure for B/N-doped graphyne, it is found that N_bB_f, B_bN_o, B_aN_e, and N_aB_g are more possible to be synthesized. For N_bB_f, after a single H_2 adsorption, it is found that the adsorption energy is 0.41 eV. In order to enhance the adsorption energy of H_2, a vertical electric field is applied on a B/C/N sheet. It is shown that the H_2 molecule is polarized under an external electric field. It can be seen that the adsorption energy increases dramatically with increasing electric field intensity. The bond length of H–H increases as the electric field increases within a certain range. The hydrogen molecules are not dissociated and are all stored in a molecular form.

Acknowledgements

This work is supported by the National Natural Science Foundation of China (Grant no. 21376013).

References

1 J. Alper, *Science*, 2003, **299**, 1686–1687.
2 R. D. Cortright, R. R. Davda and J. A. Dumesic, *Nature*, 2002, **418**, 964–967.
3 L. Schlapbach and A. Züttel, *Nature*, 2001, **414**, 353–358.
4 Y. Lu, R. Jin and W. Chen, *Nanoscale*, 2011, **3**, 2476–2480.
5 R. Coontz and B. Hanson, *Science*, 2004, **305**, 957.
6 C. Liu, Y. Y. Fan, M. Liu, H. T. Cong, H. M. Cheng and M. S. Dresselhaus, *Science*, 1999, **286**, 1127–1129.
7 H. Kruse and S. Grimme, *J. Phys. Chem. C*, 2009, **113**, 17006–17010.
8 A. C. Dillon and M. J. Heben, *Appl. Phys. A: Mater. Sci. Process.*, 2001, **72**, 133–142.
9 J. Zhou, Q. Wang, Q. Sun, P. Jena and X. S. Chen, *Proc. Natl. Acad. Sci. U. S. A.*, 2010, **107**, 2801–2806.
10 M. Khazaei, M. S. Bahramy, N. S. Venkataramanan, H. Mizuseki and Y. Kawazoe, *J. Appl. Phys.*, 2009, **106**, 094303.
11 L. P. Zhang, P. Wu and M. B. Sullivan, *J. Phys. Chem. C*, 2011, **115**, 4289–4296.

12 J. Wang, C. H. Lee and Y. K. Yap, *Nanoscale*, 2010, **2**, 2028–2034.
13 R. Ma, Y. Bando, H. Zhu, T. Sato, C. Xu and D. Wu, *J. Am. Chem. Soc.*, 2002, **124**, 7672–7673.
14 C. C. Tang, Y. Bando, T. Sato, K. Kurashima, X. X. Ding, Z. W. Gan and S. R. Qi, *Appl. Phys. Lett.*, 2002, **80**, 4641–4643.
15 J. Niu, B. K. Rao and P. Jena, *Phys. Rev. Lett.*, 1992, **68**, 2277.
16 M. Yoon, S. Yang, C. Hicke, E. Wang, D. Geohegan and Z. Zhang, *Phys. Rev. Lett.*, 2008, **100**, 206806.
17 W. Liu, Y. H. Zhao, J. Nguyen, Y. Li, Q. Jiang and E. J. Lavernia, *Carbon*, 2009, **47**, 3452–3460.
18 W. Liu, Y. H. Zhao, Y. Li, Q. Jiang and E. J. Lavernia, *J. Phys. Chem. C*, 2009, **113**, 2028–2033.
19 S. Shi, J. Y. Hwang, X. Li, X. Sun and B. I. Lee, *Int. J. Hydrogen Energy*, 2010, **35**, 629–631.
20 R. H. Baughman, H. Eckhardt and M. Kertesz, *J. Chem. Phys.*, 1987, **87**, 6687–6699.
21 N. Narita, S. Nagai, S. Suzuki and K. Nakao, *Phys. Rev. B: Condens. Matter Mater. Phys.*, 1998, **58**, 11009.
22 L. D. Pan, L. Z. Zhang, B. Q. Song, S. X. Du and H. J. Gao, *Appl. Phys. Lett.*, 2011, **98**, 173102.
23 M. Long, L. Tang, D. Wang, Y. Li and Z. Shuai, *ACS Nano*, 2011, **5**, 2593–2600.
24 G. Li, Y. Li, H. Liu, Y. Guo, Y. Li and D. Zhu, *Chem. Commun.*, 2010, **46**, 3256–3258.
25 B. Delley, *J. Chem. Phys.*, 1990, **92**, 508–517.
26 B. Delley, *J. Chem. Phys.*, 2000, **113**, 7756–7764.
27 J. P. Perdew and Y. Wang, *Phys. Rev. B: Condens. Matter Mater. Phys.*, 1992, **45**, 13244–13249.
28 Y. Okamoto and Y. Miyamoto, *J. Phys. Chem. B*, 2001, **105**, 3470–3474.
29 J. I. Martínez, I. Cabria, M. J. López and J. A. Alonso, *J. Phys. Chem. C*, 2009, **113**, 939–941.
30 Z. M. Ao, Q. Jiang, R. Q. Zhang, T. T. Tan and S. Li, *J. Appl. Phys.*, 2009, **105**, 074307.
31 Y. V. Shtogun and L. M. Woods, *J. Phys. Chem. C*, 2009, **113**, 4792–4796.
32 F. Ortmann, F. Bechstedt and W. G. Schmidt, *Phys. Rev. B: Condens. Matter Mater. Phys.*, 2006, **73**, 205101.
33 S. F. Boys and F. Bernardi, *Mol. Phys.*, 1970, **19**, 553–566.
34 I. Cabria, M. J. López and J. A. Alonso, *J. Chem. Phys.*, 2008, **128**, 144704.
35 X. Deng, M. Si and J. Dai, *J. Chem. Phys.*, 2012, **137**, 201101.
36 B. Kiran, A. K. Kandalam and P. Jena, *J. Chem. Phys.*, 2006, **124**, 224703.
37 J. H. Guo, W. D. Wu and H. Zhang, *Struct. Chem.*, 2009, **20**, 1107–1113.